

Synthesis, Characterization, and Single-Crystal EPR Studies of Three Dinuclear Copper(II) Complexes and One Mixed-Valence Tetranuclear Copper(I)–Copper(II) Cluster with an Asymmetric Imidazole-Containing Tripodal Ligand with Copper(II)–Copper(II) Distances between 3.35 and 3.63 Å

G. J. Anthony A. Koolhaas, Willem L. Driessen,* Jan Reedijk, Jacob L. van der Plas, and Rudolf A. G. de Graaff

Leiden Institute of Chemistry, Gorlaeus Laboratories, Leiden University, P.O. Box 9502, 2300 RA Leiden, The Netherlands

Dante Gatteschi

Departmento di Chimica, Università degli studi di Firenze, Via Maragliano, 75/77, I-50144 Florence, Italy

Huub Kooijman and Anthony L. Spek

Bijvoet Center for Biomolecular Research, Utrecht University, Padualaan 8, 3584 CH Utrecht, The Netherlands

Received August 24, 1995[⊗]

The synthesis and characterization of three dinuclear copper(II) complexes and one mixed-valence tetranuclear cluster with the asymmetric imidazole-containing ligand bis(1,1'-imidazole-2-yl)(4-imidazole-4(5)-yl)-2-azabutane (biib) are described. X-ray crystallographic parameters for the copper complexes are as follows. $[\text{Cu}_2(\text{biib})_2(\text{BF}_4)_2](\text{BF}_4)_2(\text{H}_2\text{O})_4$: triclinic, space group $P\bar{1}$, $a = 10.178(1)$ Å, $b = 9.4881(9)$ Å, $c = 11.037(1)$ Å, $\alpha = 95.130(10)^\circ$, $\beta = 112.20(1)^\circ$, $\gamma = 92.142(9)^\circ$, and $Z = 1$. $[\text{Cu}_2(\text{biib})_2(\text{NO}_3)_2](\text{NO}_3)_2(\text{H}_2\text{O})_4$: monoclinic, space group $P2_1/n$, $a = 9.207(6)$ Å, $b = 17.0516(6)$ Å, $c = 12.6107(7)$ Å, $\beta = 109.82(1)^\circ$, and $Z = 2$. $[\text{Cu}_2(\text{biib})_2(\text{CuBr}_3)_2]$: monoclinic, space group $P2_1/c$, $a = 11.583(2)$ Å, $b = 11.864(2)$ Å, $c = 16.070(2)$ Å, $\beta = 112.459(12)^\circ$, and $Z = 2$. The two Cu(II) ions in all four complexes are coordinated in a square-pyramidal geometry by three imidazole nitrogens and one amine nitrogen donor in the equatorial plane, and each copper ion is weakly coordinated at the axial position by respectively a tetrafluoroborate, a perchlorate, a nitrate, or a tribromocuprate(I) anion. By comparison of the structural data of the four complexes a relationship has been established between the donor strength of the anion and some structural features, like the Cu(II)–Cu(II) distance, of the dinuclear Cu(II)–Cu(II) unit in the four complexes. Single-crystal EPR spectra of $[\text{Cu}_2(\text{biib})_2(\text{BF}_4)_2](\text{BF}_4)_2(\text{H}_2\text{O})_4$ were recorded at room temperature at X-band frequencies. The triplet spectra have been fit with nonparallel **g** and **D** tensors, whose principle values are as follows: $g_{xx} = 2.022(8)$, $g_{yy} = 2.060(7)$, $g_{zz} = 2.211(8)$, $D_{x'x'} = -0.0182(9)$ cm⁻¹, $D_{y'y'} = -0.081(6)$ cm⁻¹, $D_{z'z'} = 0.0264(7)$ cm⁻¹. The compounds were further characterized and studied by ligand field and by frozen-solution and polycrystalline powder EPR spectroscopy. EPR spectra recorded at 77 K of frozen solutions of the perchlorate complex show that upon dilution in methanol the dinuclear complex reacts to form a mononuclear species.

Introduction

Copper ions, as centers of the active site of metalloproteins, play an essential role in biological processes,¹ such as electron transfer, oxidation, and dioxygen transport. In copper proteins, the copper ions are coordinated by donor atoms of the side chains of amino acid residues. Except for the Cu(I) metallothioneins, all copper proteins studied so far contain one or more imidazole residues of histidine, bound to the copper ion.

In the dinuclear type(III) copper protein hemocyanin, which functions as the dioxygen carrier for mollusks and arthropods, each copper ion is bound by three imidazole nitrogens. The

crystal structures of both the oxy- and deoxyform of some hemocyanins have been determined.² The Cu–Cu distance in the oxyform of *Limulus lyphemus* hemocyanin has been reported to be 3.55 Å and about 4.6 Å in the deoxyform.

Many model compounds have been synthesized, which are aimed to mimic the active site of certain copper proteins.^{3–8} As yet, the relation between structure and function of the active site of most copper proteins is not fully understood.

[⊗] Abstract published in *Advance ACS Abstracts*, February 15, 1996.

(1) (a) Solomon, E. I.; Hemming, B. L.; Root, D. E. In: *Bioinorganic Chemistry of Copper*; Karlin K. D., Tyeklar Z., Eds.; Chapman & Hall: London, 1993. (b) *Metal Ions in Biological Systems*; Sigel, H., Ed.; Marcel Dekker Inc.: New York, 1981.

(2) (a) Magnus, K. A.; Ton-That, H.; Carpenter, J. *Chem. Rev.* **1994**, *94*, 727. (b) Magnus, K. A.; Hazes, B.; Ton-That, H.; Bonaventura, C.; Bonaventura, J.; Hol, W. G. J. *Proteins* **1994**, *19*, 302.
(3) Kitajima, N.; Moro-oka, Y. *Chem. Rev.* **1994**, *94*, 737.
(4) Hendriks H. M. J.; Birker, P. J. M. W. L.; van Rijn, J.; Verschoor G. C.; Reedijk, J. *Inorg. Chem.* **1982**, *21*, 2637. van Rijn J.; Reedijk, J.; Dartmann, M.; Krebs, B., *J. Chem. Soc., Dalton Trans.* **1987**, 2579.
(5) Wei, N.; Murthy, N. N.; Tyeklar, Z.; Karlin, K. D. *Inorg. Chem.* **1994**, *33*, 1177.

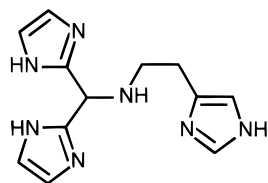


Figure 1. Schematic drawing of the ligand biib.

The ligands most frequently used in modeling dinuclear type-(III) copper proteins are benzimidazoles, pyrazoles and pyridines.³ Because of the presence of histidine as a ligand to copper ions in almost all copper proteins,¹ copper complexes with the biologically more relevant imidazolyl donors are increasingly studied as model compounds for copper protein active sites.⁵⁻⁷

In the course of our research on copper coordination compounds, both the structures and the properties of copper proteins are tried to be mimicked by modeling the active site of these proteins with imidazole containing ligands. To model the type-3 site of copper proteins, the asymmetric tripodal ligand biib (Figure 1) has been synthesized.⁷⁻⁹

Reaction of biib with copper(II) salts in ethanol results in the formation of quite unusual dinuclear and tetranuclear complexes. The dinuclear unit in the four complexes is formed by the sharing of two ligands by two copper ions. A preliminary analysis of the crystal structure and the spectroscopic properties of the dinuclear perchlorate complex have been reported before.⁷

In this paper the synthesis, crystal structures, single-crystal EPR studies, and other spectroscopic properties of the four complexes are described, and the influence of the donor strength of the axially coordinated anion on the structure and EPR spectra of the complexes is discussed in detail.

Experimental Section

Synthesis. All chemicals were commercially available, of sufficient purity. The ligand biib was prepared using the following procedure. To a solution of the freshly prepared hydrochloride salt of bis(imidazol-2-yl)nitromethane^{7,8} (3.0 g, 13.1 mmol) and histamine·2HCl (2.4 g, 13.1 mmol) in 12 mL of water was added 5.4 mL of 10 M sodium hydroxide solution, the solution was warmed to 80 °C, and to the clear solution was added 6 mL of a saturated aqueous sodium chloride solution. The solution was stirred for 45 min at 80 °C. The solvent was removed in vacuum (12 mmHg) until precipitation occurred. After 2 days, during which the product crystallized from the reaction mixture, the ligand biib was filtered from the reaction mixture, washed with water, and dried in air. Yield: 2.4 g, 72%. ¹H NMR (200 MHz, DCl 1 M, 25 °C, 0–10 ppm): δ = 8.25 (s, 1H; Im-H), 7.20 (s, 4H; Im-H), 6.93 (s, 1H; Im-H) 5.68 (s, 1H, CH), 2.65 (s (broad), 4H, CH₂).

The coordination compounds with general formula [Cu₂(biib)₂(A)₂](A)₂·xH₂O (x = 2,4), A = ClO₄⁻, BF₄⁻, and NO₃⁻, were prepared by dissolving the appropriate hydrated metal salt (1 mmol) in 10 mL of hot ethanol (96%) and adding this solution to a solution of the ligand biib (1 mmol) in 10 mL of hot ethanol (96%). After 1 week the crystalline products were collected by filtration, washed with ethanol and dried in air. The compound [Cu₂(biib)₂(CuBr₃)₂] was prepared by dissolving CuBr₂ (2 mmol) in 10 mL of hot ethanol (96%) and adding this solution to a solution of the ligand biib (1 mmol) in 10 mL of hot ethanol (96%). After 2 weeks the crystalline product was collected by filtration, washed with ethanol and dried in air. Anal. Calcd for [Cu₂(biib)₂(BF₄)₂](BF₄)₂(H₂O)₄: C, 27.17; H, 3.61; N, 18.48. Found:

Table 1. Experimental Data for the Crystallographic Analysis of the Copper Complexes

C ₂₄ H ₃₀ Cu ₂ B ₂ F ₈ N ₁₄ ·2BF ₄ ·4H ₂ O			
a, Å	10.178(1)	space group	P1̄ (No. 2)
b, Å	9.4881(9)	temp, K	297
c, Å	11.037(1)	radiation (λ, Å)	Mo Kα (0.710 73 (graphite monochromator))
α, deg	95.13(1)	d _{calcd} , g cm ⁻³	1.7842(3)
β, deg	112.20(1)	μ, cm ⁻¹	12.2 (Mo Kα)
γ, deg	92.142(9)	R _F ^a	0.044
V, Å ³	979.95(18)	R _{wF} ^b	0.047
Z	1		
MW	1052.9		
C ₂₄ H ₃₀ Cu ₂ N ₁₆ O ₆ ·2NO ₃ ·4H ₂ O			
a, Å	9.207(6)	temp, K	297
b, Å	17.0516(6)	radiation (λ, Å)	Mo Kα (0.710 73 (graphite monochromator))
c, Å	12.6107(7)	d _{calcd} , g cm ⁻³	1.7040 g cm ⁻³
β, deg	109.82(1)	μ, cm ⁻¹	12.4 (Mo Kα)
V, Å ³	1862.5(12)	R _F ^a	0.042
Z	2	R _{wF} ^b	0.041
MW	955.72		
space group	P2 ₁ /n		
	(No. 14)		
C ₂₄ H ₃₀ Br ₆ Cu ₄ N ₁₄ c			
a, Å	11.583(2)	temp, K	295
b, Å	11.864(2)	radiation (λ, Å)	Cu Kα ((Ni-filtered)
c, Å	16.070(2)		1.541 84)
β, deg	112.459(12)	d _{calcd} , g cm ⁻³	2.031 ^a g cm ⁻³
V, Å ³	2040.9(6)	μ, cm ⁻¹	95.3 ^a (Cu Kα)
Z	2	R _F ^a	0.045 for 3336 F _o > 4σ(F _o)
MW	1248.20 ^c	R _{wF} ^b	0.124
space group	P2 ₁ /c		
	(No. 14)		

$$^a R_F = \frac{\sum ||F_o| - |F_c||}{\sum |F_o|}, \quad ^b R_{wF} = \frac{[\sum w(|F_o| - |F_c|)^2 / \sum w(F_o^2)]^{1/2}}{[\sum w(F_o^2)]^{1/2}}$$

^c Without disordered solvent contribution. ^d wR2 = $[\sum [w(F_o^2 - F_c^2)^2] / \sum [w(F_o^2)^2]]^{1/2}$.

C, 27.65; H, 3.71; N, 18.64. Anal. Calcd for [Cu₂(biib)₂(NO₃)₂](NO₃)₂(H₂O)₄: C, 29.98; H, 3.98; N, 26.21. Found: C, 30.63; H, 3.93; N, 25.88.

A difference Fourier of [Cu₂(biib)₂(CuBr₃)₂] (see below) revealed a number of residual density peaks; a total number of 44 electrons were found. The residual electron density is probably caused by a mixture of water and ethanol, which were used in the synthesis and the crystallization. Found: C, 24.03; H, 2.97; N, 14.84. Anal. Calcd for [Cu₂(biib)₂(CuBr₃)₂](EtOH)(H₂O): C, 23.80; H, 2.92; N, 14.94.

Crystallography. Crystal data for the copper complexes are collected in Table 1. Crystal data for [Cu₂(biib)₂(ClO₄)₂](ClO₄)₂(H₂O)₂ have been previously reported.⁷

Neutral-atom scattering factors and anomalous dispersion factors were taken from the ref 10. Geometrical calculations were performed with PLATON.¹¹

[Cu₂(biib)₂(BF₄)₂](BF₄)₂(H₂O)₄ and [Cu₂(biib)₂(NO₃)₂](NO₃)₂(H₂O)₄ were obtained as dark blue block-shaped crystals. The diffraction data were collected on an Enraf-Nonius CAD4 diffractometer. Accurate unit-cell parameters and an orientation matrix were determined by least-squares refinement of the setting angles of 25 well-centered reflections (SET4), in the range 10.0° < θ < 12.0°. Data were collected at room temperature in ω / 2θ scan mode. Scan angle was Δω = 1.0 + 1.0 tan θ. Intensity data of 12032 and 8126 independent reflections in the range (2.0° ≤ θ ≤ 39.9°) and (2.1° ≤ θ ≤ 35°) were measured for [Cu₂(biib)₂(BF₄)₂](BF₄)₂(H₂O)₄ and [Cu₂(biib)₂(NO₃)₂](NO₃)₂(H₂O)₄, respectively. Data were corrected for Lorentz polarisation and for a linear decay of 3%. The structures were determined from the copper position (Xtal 3.2)¹² and the AUTOFOR¹³ routines. The structures were refined using Xtal 3.2.¹² Most hydrogen atoms were located on

- (6) (a) Sorrell, T. N.; Garrity, M. L.; Richards, J. L.; White, P. S. *Inorg. Chim. Acta* **1994**, *218*, 103. (b) Lynch, W. E.; Kurtz, D. M., Jr.; Wang, S.; Scott, R. A. *J. Am. Chem. Soc.* **1995**, *116*, 11030. (c) Sorrell, T. N.; Allen, W. E.; White, P. S. *Inorg. Chem.* **1995**, *34*, 952.
 (7) Koolhaas, G. J. A. A.; Driessen, W. L.; Reedijk, J.; Kooijman, H.; Spek, A. L. *J. Chem. Soc., Chem. Commun.* **1995**, 517.
 (8) Joseph, M.; Leigh T.; Swain M. L. *Synthesis* **1977**, 459.
 (9) Mulliez, E. *Tetrahedron Lett.* **1989**, *45*, 6169.

- (10) Wilson, A. J. C., Ed. *International tables for X-ray Crystallography*; Kluwer Academic Publishers: Dordrecht, The Netherlands 1992; Vol. C.
 (11) Spek, A. L. *Acta Crystallogr.* **1990**, *A46*, C34.
 (12) Hall, S. R.; Flack, H. D.; Stewart, J. M. *XTAL3.2 User's Manual*; Universities of Western Australia and Maryland: Nedlands, Australia, and College Park, MD, 1992.

the difference Fourier maps and subsequently included in the refinement. For $[\text{Cu}_2(\text{biib})_2(\text{BF}_4)_2](\text{BF}_4)_2(\text{H}_2\text{O})_4$ no hydrogen atoms could be identified on the water molecules. For $[\text{Cu}_2(\text{biib})_2(\text{NO}_3)_2](\text{NO}_3)_2(\text{H}_2\text{O})_4$ only one water hydrogen atom could be identified. All non-hydrogen atoms were refined with anisotropic thermal parameters. The hydrogen atoms were refined isotropically. For $[\text{Cu}_2(\text{biib})_2(\text{BF}_4)_2](\text{BF}_4)_2(\text{H}_2\text{O})_4$ convergence was reached at $R_F = 0.044$, $R_{wF} = 0.047$, $w = 1/\sigma^2(F)$, and $S = 2.256$ for 349 parameters and 6432 reflections with $I > 2\sigma(I)$. No residual density was found outside -1.84 and $+0.86 \text{ e } \text{Å}^{-3}$. For $[\text{Cu}_2(\text{biib})_2(\text{NO}_3)_2](\text{NO}_3)_2(\text{H}_2\text{O})_4$ convergence was reached at $R_F = 0.042$, $R_{wF} = 0.041$, $w = 1/\sigma^2(F)$, and $S = 1.66$ for 288 parameters and 3395 reflections with $I > 2\sigma(I)$. No residual density was found outside -2.8 and $+1.1 \text{ e } \text{Å}^{-3}$.

$[\text{Cu}_2(\text{biib})_2(\text{CuBr}_3)_2]$ was obtained as dark blue, plate-shaped crystals of approximate dimensions $0.3 \times 0.3 \times 0.1 \text{ mm}$ suitable for X-ray structure determination which were mounted on a Lindemann-glass capillary and transferred to an Enraf-Nonius CAD4F sealed tube diffractometer. Accurate unit-cell parameters and an orientation matrix were determined by least-squares refinement of the setting angles of 25 well-centered reflections (SET4), in the range $16.9^\circ < \theta < 23.8^\circ$. The unit-cell parameters were checked for the presence of higher lattice symmetry.¹⁴ Data were collected at room temperature in $\omega/2\theta$ scan mode. Scan angle was $\Delta\omega = 0.65 + 0.14 \tan \theta$. Intensity data of 4363 reflections in the range $2.98^\circ \leq \theta \leq 74.98^\circ$ were measured, of which 4003 were independent ($R_{\text{int}} = 0.041$). Data were corrected for Lorentz and polarization effects. Three periodically measured reflections showed no significant decay during 35 h of X-ray exposure time. An empirical absorption correction was applied (DIFABS,¹⁵ correction range 0.36–2.50). The structure was solved by automated Patterson methods and subsequent difference Fourier techniques (SHELXS86).¹⁶ Refinement on F^2 was carried out using full-matrix least-squares techniques (SHELXL93);¹⁷ no observance criterion was applied during refinement. Hydrogen atoms (including the amine and imidazole hydrogen atoms) were included in the refinement on calculated positions riding on their carrier atoms. After anisotropic refinement of the non-hydrogen atoms and introduction of the hydrogen atoms at expected positions a $wR2$ value of 0.222 ($R_F = 0.086$ for 3336 $F_o > 4\sigma(F_o)$) was obtained. A difference Fourier revealed a number of residual density peaks (approximately $2.4 \text{ e } \text{Å}^{-3}$) in two symmetry related cavities $x = 1/2, y = 1/2, z = 0$ and $x = 1/2, y = 0, z = 1/2$. No discrete solvent model could be refined. The BYPASS¹⁸ procedure, as implemented in the program PLATON,¹¹ was used to take this electron density into account. A total number of 44 electrons were found in each of the two cavities, which have a volume of 124.5 Å^3 each. The cavities are probably filled with a mixture of water and ethanol, which was used in the synthesis and the crystallization. Since the boundary of the disordered solvent region is difficult to define, due to hydrogen bonding of the amine and imidazole nitrogens toward the disordered solvent, it is not possible to assess the correct occupancy of the cavity. All non-hydrogen atoms were refined with anisotropic thermal parameters, the hydrogen atoms were refined with an overall isotropic thermal parameter related to the value of the equivalent isotropic thermal parameter of their carrier atoms by a factor of 1.2. Convergence was reached at $wR2 = 0.124$, $w^{-1} = \sigma^2(F^2) + (0.0615P)^2 + 8.19P$, where $P = (\text{Max}(F_o^2, 0) + 2F_c^2)/3$, $R_F = 0.045$ (for 3336 $F_o > 4\sigma(F_o)$), and $S = 1.05$ for 217 parameters. No residual density was found outside -1.06 and $+1.07 \text{ e } \text{Å}^{-3}$.

Spectral and Magnetic Measurements. Fourier transform infrared spectra ($4000\text{--}200 \text{ cm}^{-1}$) were recorded on a Bruker IFS 113V FT-IR spectrophotometer, as KBr pellets.

Ligand-field spectra of the solids ($300\text{--}2000 \text{ nm}$) were recorded on a Perkin-Elmer 330 spectrophotometer equipped with a diffuse-reflectance attachment, using MgO as a reference.

X-band EPR spectra (powder or frozen solution) were recorded on a JEOL RE2X electron spin resonance spectrometer. Variable temperature X-band powder EPR spectra have been obtained on a JEOL RE2X electron spin resonance spectrometer using an ESR900 continuous-flow cryostat.

Single-Crystal EPR. EPR-suitable single crystals of $[\text{Cu}_2(\text{biib})_2(\text{BF}_4)_2](\text{BF}_4)_2(\text{H}_2\text{O})_4$ and $\text{Cu}_2(\text{biib})_2(\text{NO}_3)_2(\text{NO}_3)(\text{H}_2\text{O})_4$ were oriented with an Enraf-Nonius CAD4 diffractometer and were found to conform to the X-ray structures. Single crystals of $[\text{Cu}_2(\text{biib})_2(\text{BF}_4)_2](\text{BF}_4)_2(\text{H}_2\text{O})_4$ showed well-developed 001 and 010 faces. Crystals of $\text{Cu}_2(\text{biib})_2(\text{NO}_3)_2(\text{NO}_3)(\text{H}_2\text{O})_4$ were found to have a well-developed 010 face. Single-crystal X-band EPR spectra were recorded at room temperature on a Varian E-9 spectrometer.

Magnetic Measurements. Magnetic susceptibilities of the perchlorate complex were measured in the temperature range $250\text{--}4.5 \text{ K}$ with a Cryogenic S600C SQUID susceptometer. Data were corrected for diamagnetic contributions, which were estimated from the Pascal constants.

Results and Discussion

Structure of the Complexes. Structural analysis of the four complexes shows that in each complex the two Cu(II) ions are coordinated in a square-pyramidal geometry. In the equatorial plane, each copper ion is coordinated by one of the imidazole nitrogens from the bis(imidazole) unit (N(13)), the amine nitrogen (N(42)), and the nitrogen of the separate imidazole group (N(33)), while the fourth coordinated nitrogen N(23)^a is from an imidazole group provided by the bis(imidazole) unit of another ligand. Cu(II)–N distances (Table 3) are between 1.953(3) and 2.074(3) and are in the normal range for Cu(II)–imidazole or Cu(II)–amine bonds.¹⁹

In the present complexes the dinuclear Cu(II)–Cu(II) unit is formed by the sharing of two ligands by two Cu(II) ions. Similar coordination behavior of a tripodal tetradentate ligand has been reported by Karlin and co-workers⁵ in the dinuclear Cu(I) complex $[(\text{bpia})_2\text{Cu}_2](\text{CF}_3\text{SO}_3)_2$ (bpia = bis(2-pyridyl)methyl(1-methylimidazol-2-yl)methyl)amine). This dinuclear Cu(I) complex is formed by the sharing of two imidazole groups by two Cu(I) ions. A possible driving force for the dimerization of $[(\text{BPIA})_2\text{Cu}_2](\text{CF}_3\text{SO}_3)_2$ might be a stacking interaction between two pyridines of the two bpia ligands.⁵ In the present complexes no intramolecular stacking interactions are observed between the imidazole rings, and the formation of the dinuclear Cu(II) unit in complexes with the ligand biib is probably due to steric effects. Coordination chemistry studies with the ligand Htidah²⁰ (1,1,6,6-tetrakis(imidazol-2-yl)-2,5-diazahexane), which also contains the bis(imidazole)methylamine unit, revealed that due to steric reasons the bis(imidazole) methylamine unit cannot encapsulate one Cu(II) ion. Due to the same steric effects the ligand biib cannot act as a tetradentate mononucleating ligand. But upon dimerization all four nitrogen donors of the ligand biib can coordinate to the copper ions in a square-planar fashion.

In the present complexes each Cu(II) ion is coordinated at the axial position by a monodentate coordinated BF_4^- , ClO_4^- , NO_3^- , or CuBr_3^{2-} anion. The distance between the Cu(II) ion and the donor atom of the coordinated anion is as follows: 2.606(2), 2.563(3), 2.497(4), or 2.9504(11) Å, respectively. Coordination of a $[\text{CuBr}_3]^{2-}$ unit to a Cu(II) ion is quite unusual and has only been observed once before, in the tetranuclear complex $[\text{Cu}(\text{maamt})(\text{CuBr}_3)]_2$.²¹ In the latter complex the $[\text{CuBr}_3]^{2-}$ unit acts as a bridging ligand between the two Cu(II) ions. The two Cu(II)–Br distances in $[\text{Cu}(\text{maamt})(\text{CuBr}_3)]_2$ (3.116(3) and 2.960(3) Å) are both larger than the distance

(13) Kinneging, A. J.; de Graaff, R. A. G. *J. Appl. Crystallogr.* **1984**, *17*, 364.

(14) Spek, A. L. *Acta Crystallogr.* **1988**, *21*, 578.

(15) N. Walker, N.; Stewart, D. *Acta Crystallogr.* **1983**, *39*, 158.

(16) Sheldrick, G. M., SHELXS86: A program for crystal structure determination; University of Göttingen: Göttingen Germany, 1986.

(17) Sheldrick, G. M., SHELXL93 Program for crystal structure refinement; University of Göttingen: Göttingen Germany, 1993.

(18) van der Sluis, P.; Spek, A. L. *Acta Crystallogr.* **1990**, *A46*, 194.

(19) Hathaway, B. J. *Struct. Bonding* **1984**, *57*, 55.

(20) Koolhaas, G. J. A. A.; Driessen, W. L.; van Koningsbruggen, P. J.;

Reedijk, J.; Spek, A. L. *J. Chem. Soc., Dalton Trans* **1993**, 3803.

(21) van Koningsbruggen, P. J.; Haasnoot, J. G.; Kooijman, H.; Reedijk, J.; Spek, A. L. To be submitted for publication.

Table 2. Final Atomic Coordinates and Equivalent Isotropic Thermal Parameters of the Non-Hydrogen Atoms

atom	x	y	z	$U_{eq}^a, \text{\AA}^2$	atom	x	y	z	$U_{eq}^a, \text{\AA}^2$
(a) $[\text{Cu}_2(\text{biib})_2(\text{BF}_4)_2](\text{BF}_4)_2(\text{H}_2\text{O})_4$									
Cu(1)	0.33616(2)	0.05406(2)	0.92797(2)	0.0235(1)	C(35)	0.0529(2)	-0.2368(2)	0.6335(2)	0.0414(6)
N(11)	0.6341(2)	0.3778(2)	1.0168(2)	0.0332(5)	C(41)	0.5290(2)	0.1878(2)	0.8197(2)	0.0254(5)
N(13)	0.4899(2)	0.2054(2)	1.0263(2)	0.0286(4)	C(43)	0.3457(2)	0.0179(2)	0.6502(2)	0.0306(5)
N(21)	0.6959(2)	0.0733(2)	0.7316(2)	0.0325(5)	C(44)	0.1867(2)	-0.0242(2)	0.5933(2)	0.0341(6)
N(23)	0.6897(2)	-0.0098(2)	0.9089(2)	0.0287(5)	F(51)	-0.0169(2)	0.2631(2)	0.9128(2)	0.0739(6)
N(31)	0.0392(2)	-0.2791(2)	0.7439(2)	0.0443(6)	F(52)	0.0392(2)	0.4491(2)	0.8297(2)	0.0916(10)
N(33)	0.1830(2)	-0.0866(2)	0.8110(2)	0.0296(4)	F(53)	0.1841(2)	0.2720(2)	0.8732(2)	0.0737(6)
N(42)	0.3820(2)	0.1157(2)	0.7726(2)	0.0250(4)	F(54)	-0.0291(2)	0.2399(3)	0.7035(2)	0.0965(8)
C(12)	0.5531(2)	0.2597(2)	0.9538(2)	0.0262(5)	B(50)	0.0439(3)	0.3050(3)	0.8278(3)	0.0405(6)
C(14)	0.5334(2)	0.2959(2)	1.1427(2)	0.0355(6)	F(61)	0.2532(2)	0.3389(2)	0.6076(2)	0.0717(6)
C(15)	0.6233(2)	0.4019(2)	1.1371(2)	0.0393(6)	F(62)	0.4353(2)	0.4803(2)	0.6074(2)	0.0639(5)
C(22)	0.6385(2)	0.0845(2)	0.8237(2)	0.0249(5)	F(63)	0.2167(2)	0.4831(2)	0.4499(2)	0.1105(8)
C(24)	0.7832(2)	-0.0830(2)	0.8672(2)	0.0373(6)	F(64)	0.3437(3)	0.2963(3)	0.4539(3)	0.1149(12)
C(25)	0.7873(3)	-0.0314(3)	0.7593(2)	0.0393(6)	B(60)	0.3115(3)	0.4018(3)	0.5291(3)	0.0490(8)
C(32)	0.1185(2)	-0.1883(2)	0.8482(2)	0.0372(6)	O(70)	0.6372(3)	0.2505(2)	0.5368(2)	0.0680(8)
C(34)	0.1410(2)	-0.1162(2)	0.6746(2)	0.0307(5)	O(75)	0.2572(2)	0.5134(3)	0.1592(2)	0.0742(8)
(b) $[\text{Cu}_2(\text{biib})_2(\text{NO}_3)_2](\text{NO}_3)_2(\text{H}_2\text{O})_4$									
Cu	0.61565(4)	0.41290(2)	0.53586(3)	0.0188	C(22)	0.3015(3)	0.4728(2)	0.2652(2)	0.0244
O(4)	1.0077(3)	0.2816(2)	0.4691(2)	0.0571	C(24)	0.1089(4)	0.5466(2)	0.2627(3)	0.0383
O(5)	0.8285(3)	0.3241(2)	0.5302(2)	0.0518	C(25)	0.0559(4)	0.4970(2)	0.1749(3)	0.0408
O(10)	0.8273(4)	0.3534(2)	0.3632(2)	0.0834	C(32)	0.5690(4)	0.3224(2)	0.7201(3)	0.0306
N(3)	0.8875(3)	0.3198(2)	0.4530(2)	0.0373	C(34)	0.4602(4)	0.2624(2)	0.5610(3)	0.0295
N(11)	0.6452(3)	0.5414(2)	0.2788(2)	0.0308	C(35)	0.4295(4)	0.2209(2)	0.6426(3)	0.0377
N(13)	0.6648(3)	0.4946(2)	0.4449(2)	0.0270	C(41)	0.4577(3)	0.4352(2)	0.2898(2)	0.0259
N(21)	0.1784(3)	0.4506(2)	0.1776(2)	0.0332	C(43)	0.3571(4)	0.3166(2)	0.3618(3)	0.0320
N(23)	0.2642(3)	0.5322(2)	0.3200(2)	0.0276	C(44)	0.4138(4)	0.2455(2)	0.4382(3)	0.0358
N(31)	0.4992(3)	0.2588(2)	0.7420(2)	0.0359	O(3)	0.1389(3)	0.0945(2)	0.6049(2)	0.0561
N(33)	0.5488(3)	0.3266(2)	0.6110(2)	0.0274	O(7)	0.1909(3)	0.0706(2)	0.4530(2)	0.0634
N(42)	0.4895(3)	0.3711(2)	0.3768(2)	0.0256	O(8)	-0.0450(3)	0.0881(2)	0.4450(2)	0.0573
C(12)	0.5874(3)	0.4913(2)	0.3355(2)	0.0239	N(1)	0.0976(3)	0.0842(2)	0.5023(2)	0.0412
C(14)	0.7804(4)	0.5504(2)	0.4589(3)	0.0337	O(9)	0.2534(3)	0.3481(2)	0.0371(2)	0.0598
C(15)	0.7670(4)	0.5804(2)	0.3565(3)	0.0362	O(6)	0.5806(4)	0.2520(2)	0.2239(3)	0.0821
(c) $(\text{CuBr}_3)_2$									
Br(1)	0.50473(5)	0.32465(6)	0.42478(4)	0.0420(2)	C(12)	0.2213(4)	-0.0230(4)	0.1090(3)	0.0209(12)
Br(2)	0.48048(7)	0.21402(8)	0.18644(6)	0.0632(3)	C(14)	0.1197(5)	-0.0668(5)	0.1930(4)	0.0322(17)
Br(3)	0.15092(5)	0.28361(5)	0.21414(4)	0.0382(2)	C(15)	0.2258(6)	-0.1292(5)	0.2213(4)	0.0372(17)
Cu(1)	0.02639(6)	0.13428(6)	0.05872(5)	0.0214(2)	C(22)	0.2172(4)	-0.0228(4)	-0.0480(3)	0.0211(12)
Cu(2)	0.36984(9)	0.27128(9)	0.27755(7)	0.0503(3)	C(24)	0.1325(5)	-0.1291(5)	-0.1656(3)	0.0309(17)
N(11)	0.2887(4)	-0.1004(4)	0.1675(3)	0.0303(12)	C(25)	0.2358(5)	-0.0798(5)	-0.1724(4)	0.0326(17)
N(13)	0.1173(4)	-0.0003(4)	0.1220(3)	0.0247(12)	C(32)	-0.1690(5)	0.3030(5)	-0.0318(4)	0.0346(17)
N(21)	0.2866(4)	-0.0149(3)	-0.0985(3)	0.0258(12)	C(34)	0.0030(5)	0.3423(4)	-0.0519(3)	0.0317(16)
N(23)	0.1227(4)	-0.0928(3)	-0.0869(3)	0.0229(12)	C(35)	-0.0849(6)	0.4226(5)	-0.0954(4)	0.0384(17)
N(31)	-0.1893(5)	0.3966(4)	-0.0799(3)	0.0396(16)	C(41)	0.2516(4)	0.0393(4)	0.0390(3)	0.0209(12)
N(33)	-0.0523(4)	0.2663(3)	-0.0128(3)	0.0252(12)	C(43)	0.1813(6)	0.2167(4)	-0.0490(4)	0.0335(17)
N(42)	0.1849(4)	0.1498(3)	0.0302(3)	0.0229(12)	C(44)	0.1354(6)	0.3351(4)	-0.0428(4)	0.0375(16)

^a $U_{eq} = 1/3$ of the trace of the orthogonalized U.

(2.9504(11) Å) observed in the present complex. The coordination around the Cu(I) ion in the present complex can best be described as distorted trigonal planar. The deviation of the Cu(I) ion from the plane provided by the three coordinated bromides is 0.0614(11) Å. The observed angles around the Cu(I) ion are as follows: Br(1)–Cu(2)–Br(2) = 112.66(5)°, Br(1)–Cu(2)–Br(3) = 127.40(5)°, and Br(2)–Cu(2)–Br(3) = 119.74(5)°.

No intermolecular stacking interactions or short intermolecular Cu–Cu contacts are observed in the four complexes. The smallest intermolecular Cu(II)–Cu(II) distances observed in the four complexes (BF_4^- , ClO_4^- , NO_3^- , CuBr_3^{2-}) are, respectively, 7.6416(8), 7.4124(7), 8.0045(5), and 8.4912(18) Å. The smallest intermolecular Cu(II)–Cu(I) distance in the tribromocuprate(I) complex is 7.1576(18) Å.

The general solid-state structure of the cationic complexes $[\text{Cu}_2(\text{biib})_2\text{A}_2]^{2+}$ (A = BF_4^- , ClO_4^- , NO_3^- , and CuBr_3^{2-}) is shown in Figure 2 (PLUTON²² projection). The structure of the mixed-valence tetranuclear cluster (TME projection¹¹) is shown in Figure 3. Selected bond distances and angles are listed in Table 2.

Comparison of the Structure of the Four Complexes. The X-ray data sets of all four complexes were obtained at room temperature, which allows a detailed structural comparison of the complexes. Apparently a relationship exists between the donor strength of the anion and some structural features of the dinuclear unit of the complexes, *i.e.* the Cu(II)–Cu(II) distance, the distance of the copper(II) ion to the least-squares plane provided by N(13), N(42), N(33), and N(23)^a, and the distance between the two inversion-related ($-x$, $-y$, $-z$), and therefore parallel, least-squares planes. A schematic representation of the influence of the anion on the structure of the dinuclear Cu(II)–Cu(II) unit is shown in Figure 4, the selected structural parameters are listed in Tables 3 and 4.

The binding properties of the coordinated anions in the four complexes are known to increase in the following order:²³ $\text{BF}_4^- < \text{ClO}_4^- < \text{NO}_3^-$. Although the donor properties of the

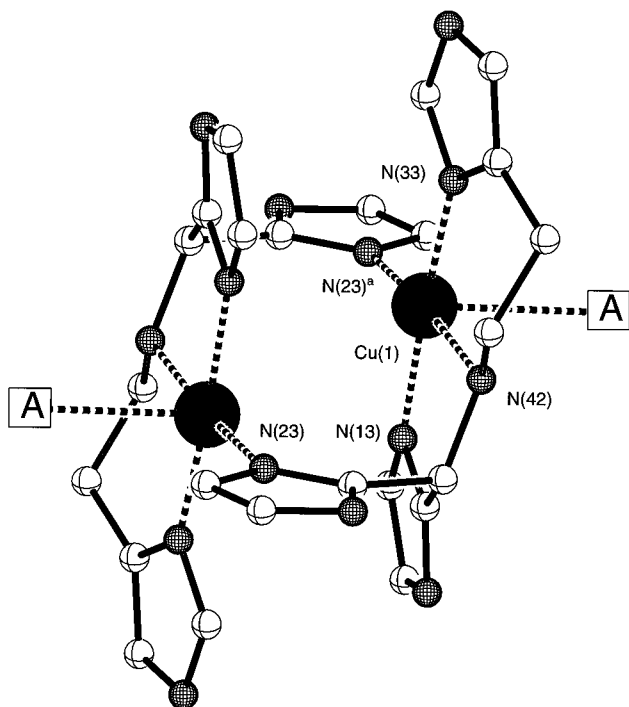
(22) Spek, A. L. *PLUTON Molecular graphics program*; Utrecht University: The Netherlands, 1995.

(23) Linert, W.; Jameson, R. F.; Taha, A. *J. Chem. Soc., Dalton Trans.* **1993**, 318.

Table 3. Selected Bond Distances (Å) and Angles (deg) for the Copper Complexes^a

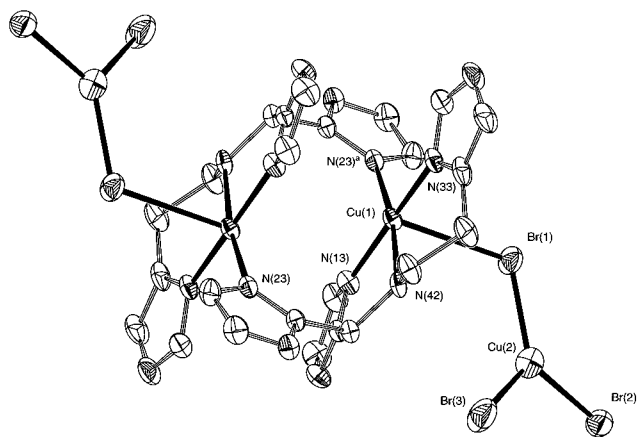
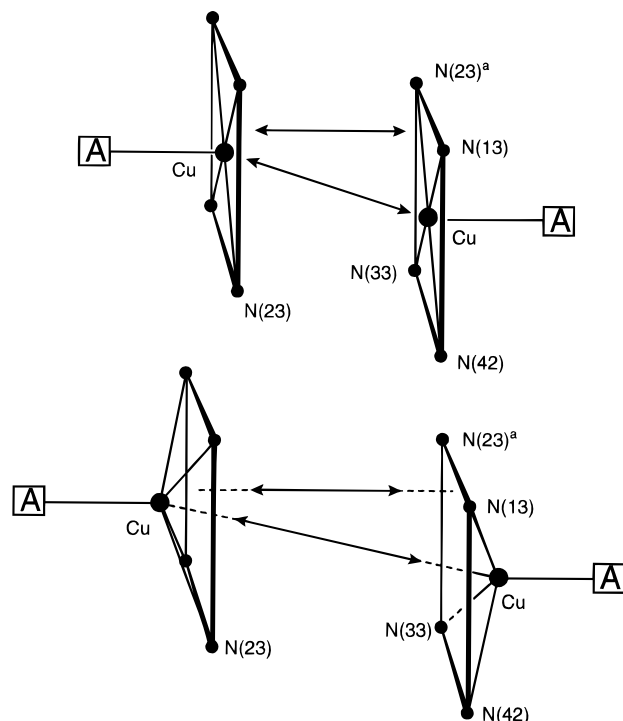
	BF ₄ ⁻	ClO ₄ ⁻	NO ₃ ⁻	CuBr ₃ ²⁻
Cu(1)–N(13)	1.990(2)	1.980(3)	1.953(3)	1.968(5)
Cu(1)–N(33)	1.973(2)	1.954(3)	1.959(3)	1.951(4)
Cu(1)–N(42)	2.065(2)	2.060(3)	2.074(3)	2.063(5)
Cu(1)–N(23) ^a	1.993(2)	2.004(3)	2.010(3)	2.007(5)
Cu(1)–A ^b	2.606(2)	2.563(3)	2.497(4)	2.9504(11)
Cu(1)–Cu(1) ^a	3.3532(4)	3.4229(6)	3.5875(5)	3.6340(12)
Br(1)–Cu(2)				2.3697(13)
Br(2)–Cu(2)				2.3835(15)
Br(3)–Cu(2)				2.3485(13)
Cu(1)–Cu(2)				4.4884(15)
N(13)–Cu(1)–N(33)	173.09(8)	173.69(14)	173.42(11)	173.3(2)
N(13)–Cu(1)–N(42)	81.10(8)	80.91(12)	80.93(12)	80.87(18)
N(13)–Cu(1)–N(23) ^a	92.45(8)	91.16(12)	91.88(12)	91.21(19)
N(33)–Cu(1)–N(42)	92.20(8)	92.79(12)	92.57(12)	93.02(18)
N(23) ^a –Cu(1)–N(33)	94.27(8)	95.14(12)	94.55(12)	94.66(19)
N(23) ^a –Cu(1)–N(42)	173.52(8)	172.00(10)	172.19(13)	170.91(15)
X–Cu(1)–N(13)	81.99(8)	90.88(11)	94.32(11)	93.31(14)
X–Cu(1)–N(33)	95.22(8)	87.88(11)	86.37(12)	89.08(13)
X–Cu(1)–N(42)	79.57(7)	81.94(11)	87.22(10)	86.89(12)
X–Cu(1)–N(23) ^a	100.16(8)	97.29(11)	96.41(11)	98.09(12)
Br(1)–Cu(2)–Br(2)				112.66(5)
Br(1)–Cu(2)–Br(3)				127.40(5)
Br(2)–Cu(2)–Br(3)				119.74(5)
Cu(1)–Br(3)–Cu(2)				115.31(4)

^a Key: (a) denotes symmetry operation $-x, -y, -z$; (b) denotes the coordinating atom of BF₄⁻, ClO₄⁻, NO₃⁻, and CuBr₃²⁻.

**Figure 2.** General solid-state structure of the copper complexes (PLUTON²² projection). Hydrogen atoms and noncoordinated anions are omitted for clarity (A = BF₄⁻, ClO₄⁻, NO₃⁻, and CuBr₃²⁻).

CuBr₃²⁻ anion have never been fully investigated, the donor strength is expected to be similar to a bromide anion (*i.e.* > NO₃⁻). The difference in donor strength between a perchlorate and tetrafluoroborate anion is known to be very small or even neglectable.²³

In the tetrafluoroborate and perchlorate complex the Cu–Cu distances are, respectively, 3.3532(4) and 3.4229(6) Å. In both complexes no significant deviations of the copper ion from the least-squares plane provided by the four coordinated nitrogen atoms are observed, *i.e.* 0.010(1) Å in the tetrafluoroborate and 0.012(1) Å in the perchlorate complex. The distance between the two least-squares planes is 2.990(2) and 2.933(3) Å,

**Figure 3.** TME plot¹¹ of the mixed-valence tetranuclear copper complex [Cu₂(biib)₂(CuBr₃)₂], drawn at 50% probability. Hydrogen atoms are omitted for clarity.**Figure 4.** Schematic representation of the influence of the donor strength of the axially coordinated anion on the solid-state structure of the dinuclear Cu(II)–Cu(II) unit. Increasing donor strength results in an increase of the Cu(II)–Cu(II) distance, the distance of the Cu(II) ion to the least-squares plane, and the distance between the two least-squares planes.

respectively. In the perchlorate complex a larger Cu(II)–Cu(II) distance, but a smaller distance between the two least-squares planes, is observed. This can be explained by a parallel shift of the four nitrogen donors defining the least-squares plane. This shift is reflected in the angle between the plane and the Cu–Cu direction. This angle is 58.2(1)°, 60.2(1)°, and 61.7(1)° in the perchlorate, nitrate, and tribromocuprate complexes, respectively, which is in agreement with the expected increase of the angle with increasing Cu(II)–Cu(II) distance, presuming that an increase of the Cu(II)–Cu(II) distance is caused by a migration of the copper ion in the molecular *z*-direction. In the tetrafluoroborate complex this angle is 62.3(1)°, which is much larger than expected. A perchlorate anion is known to provide a slightly stronger coordination than a tetrafluoroborate anion, but the small structural differences between these two complexes cannot be fully related to the small difference in

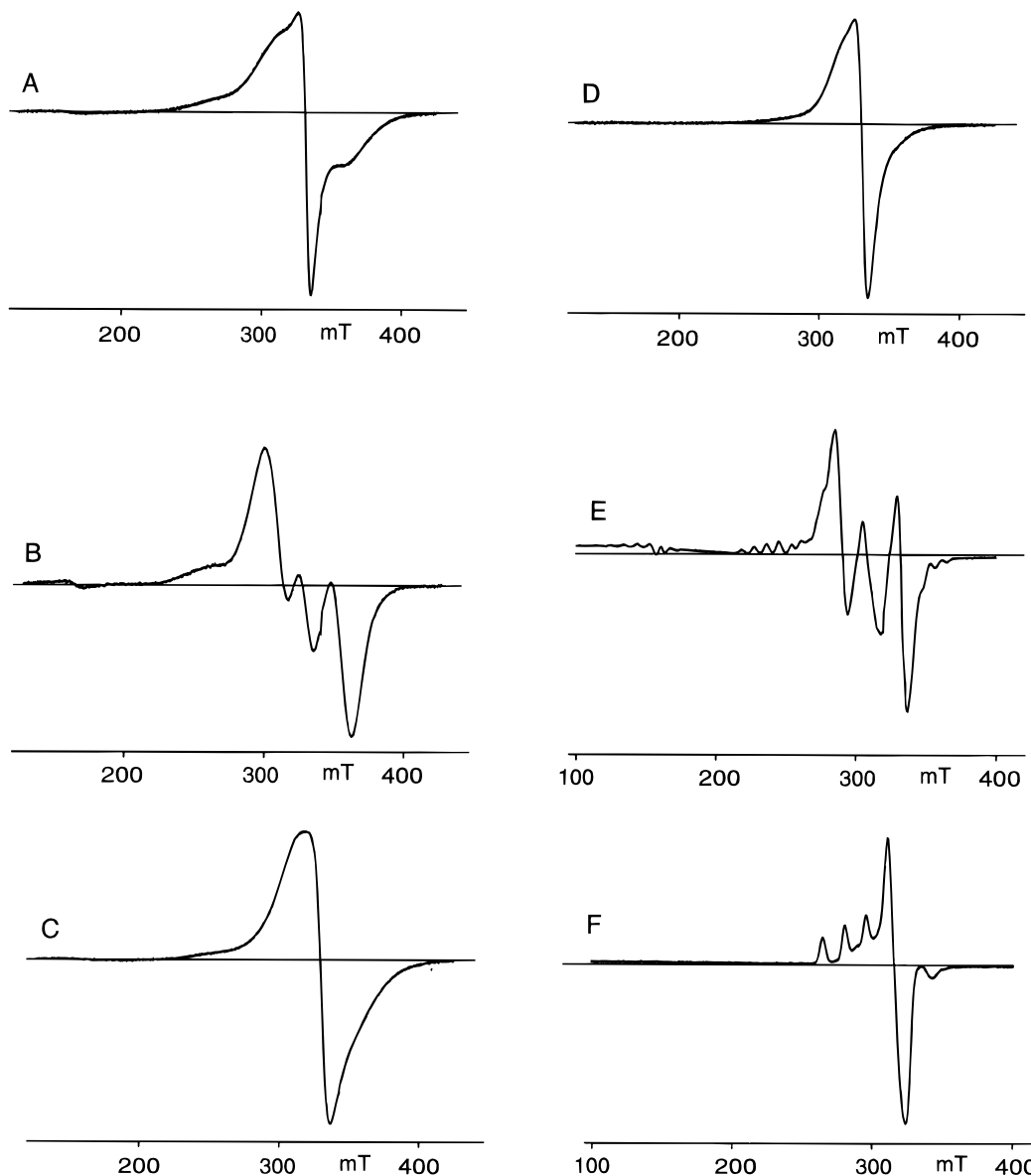


Figure 5. Polycrystalline powder EPR spectra of the copper complexes recorded at room temperature (A = BF_4^- , B = ClO_4^- , C = NO_3^- , D = CuBr_3^{2-}) and frozen solution EPR spectra of the perchlorate complex recorded at 77 K ($E = 0.01$ M in MeOH/DMSO 80/20, $F = 2 \times 10^{-4}$ M in MeOH).

Table 4. Deviations (\AA) of Cu(1) and Donor Atoms from the Least-Squares Plane Provided by N(13), N(33), N(23)^a, and N(42) (\AA), Distance (\AA) between the Symmetry-Related Least-Squares Planes Provided by N(13), N(33), N(23)^a, and N(42) (\AA), and Angle (deg) between the Plane and the Cu(II)–Cu(II) Vector

atom ^a	deviation			
	BF_4^-	ClO_4^-	NO_3^-	CuBr_3^{2-}
N(13)	0.019(2)	-0.006(3)	0.018(3)	0.017(5)
N(23) ^a	-0.017(2)	0.006(3)	-0.017(3)	-0.015(4)
N(33)	0.017(2)	-0.005(3)	0.016(3)	0.015(4)
N(42)	-0.019(2)	0.006(3)	-0.018(3)	-0.016(4)
Cu(1)	-0.010(1)	-0.012(1)	0.038(1)	0.067(1)
	BF_4^-	ClO_4^-	NO_3^-	CuBr_3^{2-}
distance	2.990(2)	2.933(3)	3.036(3)	3.066(6)
angle	62.3(1)	58.2(1)	60.2(1)	61.7(1)

^a Key: (a) denotes symmetry operation $-x$, $-y$, $-z$.

binding strength of the respective anion and might be caused by crystal-packing effects as well.

In the nitrate complex a significant effect of the coordination of the anion on the structure of the dinuclear unit of the complex is observed. The coordination of the nitrate ion causes a small

distortion of the square-pyramidal environment of the copper ion. The distance of the copper ion to the least-squares plane is 0.038(1) \AA . The copper(II) ion lies above the plane and is directed toward the oxygen donor atom of the coordinated nitrate anion. Comparison of the nitrate complex with the tetrafluoroborate and perchlorate complex shows that the coordination of the nitrate results in a larger Cu(II)–Cu(II) distance (3.5875(5) \AA), but also in a larger distance between the two parallel least-squares planes (3.036(3) \AA).

The strongest anion coordination is observed in the tribromocuprate(I) complex. This strong coordination is reflected in the distance of the copper(II) ion to the least-squares plane (0.067(1) \AA), the relatively large Cu(II)–Cu(II) distance (3.6340(12) \AA), and the distance between the two least-squares planes (3.066(6) \AA).

Polycrystalline Powder EPR. EPR spectra recorded at room temperature and 77 K of the polycrystalline powders of the present complexes, show typical axial triplet spectra^{24,25} (Figure 5A–5D). No sharpening of the lines or hyperfine splitting is observed upon cooling from room temperature to 77 K. Except for the tribromocuprate(I) complex, the half-field signal is

observed for all other complexes. The spectra contain an isotropic signal centered at $g = 2.06$, indicating crystal defects or monomeric impurities in the complexes. The EPR parameters of the perchlorate complex were determined from standard analysis of the polycrystalline powder spectrum.²⁴ Assuming that \mathbf{g} and \mathbf{D} are coincident,²⁷ $g_{\perp} = 2.02$, $g_{\parallel} = 2.21$, and $D = 0.058 \text{ cm}^{-1}$. In the polycrystalline powder EPR spectra of the nitrate and tribromocuprate(I) complex, the high intensity of the isotropic signal and the low resolution of the triplet signals make a determination of the g and D values from these spectra impossible. The g and D values of the nitrate and tetrafluoroborate complex were determined from the single-crystal EPR spectra and will be discussed below. The g and D values of the tribromocuprate(I) complex could not be determined, since no crystals suitable for a single-crystal EPR study were available.

Single-Crystal EPR. Suitable crystals for single-crystal EPR studies were obtained for the tetrafluoroborate and nitrate complex. The nitrate complex crystallizes in a monoclinic space group with two molecules in the unit cell. Single-crystal EPR spectra of the nitrate complex were recorded at X-band frequencies by rotating the crystal with respect to the static magnetic field around the three orthogonal axes a , b , and c^* . The relatively large line width caused merging of the lines arising from the two symmetry related dinuclear molecules and made a detailed analysis of the single-crystal EPR spectra impossible. Although a full analysis was impossible the g_{xy} , g_z , and D values of the nitrate complex, which could not be determined from the polycrystalline powder spectrum, could be estimated²⁵ from the single-crystal EPR spectra and are as follows: $g_{\perp} = 2.02$, $g_{\parallel} = 2.21$, and $D = 0.058 \text{ cm}^{-1}$ (assuming that \mathbf{g} and \mathbf{D} are coincident²⁶).

The tetrafluoroborate complex crystallizes in the triclinic space group $P\bar{1}$ with only one molecule in the unit cell. Single-crystal EPR spectra of the tetrafluoroborate complex were recorded at X-band by rotating the crystal with respect to the static magnetic field around the three orthogonal axes a , b^* , and c' . The b^* axis is perpendicular to the (010) face, the a axis is defined by the intersection of the (001) and (010) faces, and the c' axis is perpendicular to both the a and b^* axis. In each rotation two fine-structure lines split by the zero-field parameter D are observed. The angular dependence of the transition fields in the three rotations and the best-fit curves²⁷ are shown in Figure 6. The triplet spectra have been fit with nonparallel \mathbf{g} and \mathbf{D} tensors.^{27,28} The best-fit spin-Hamiltonian parameters, together with experimental errors, as well as the directions of the \mathbf{g} and \mathbf{D} tensors,²⁷ whose principal values are $g_{xx} = 2.022(8)$, $g_{yy} = 2.060(7)$, $g_{zz} = 2.211(8)$, $D_{x'x'} = -0.0182(9) \text{ cm}^{-1}$, $D_{y'y'} = -0.081(6) \text{ cm}^{-1}$, and $D_{z'z'} = 0.0264(7) \text{ cm}^{-1}$, are listed in Table 5. A PLUTON²² projection showing the principal directions of the \mathbf{g} and \mathbf{D} tensors is given in Figure 7.

The g_{zz} and $D_{z'z'}$ directions are not coincident, making an angle of *ca.* 23° ; g_{zz} is quasi parallel to the normal to the least-squares plane formed by N(42), N(13), N(33) and N(23a), in reasonable agreement with the expectation that the largest g value for a square pyramidal copper(II) is observed parallel to the pseudotetragonal axis.²⁵ $D_{z'z'}$ makes an angle of *ca.* 13° with the Cu–

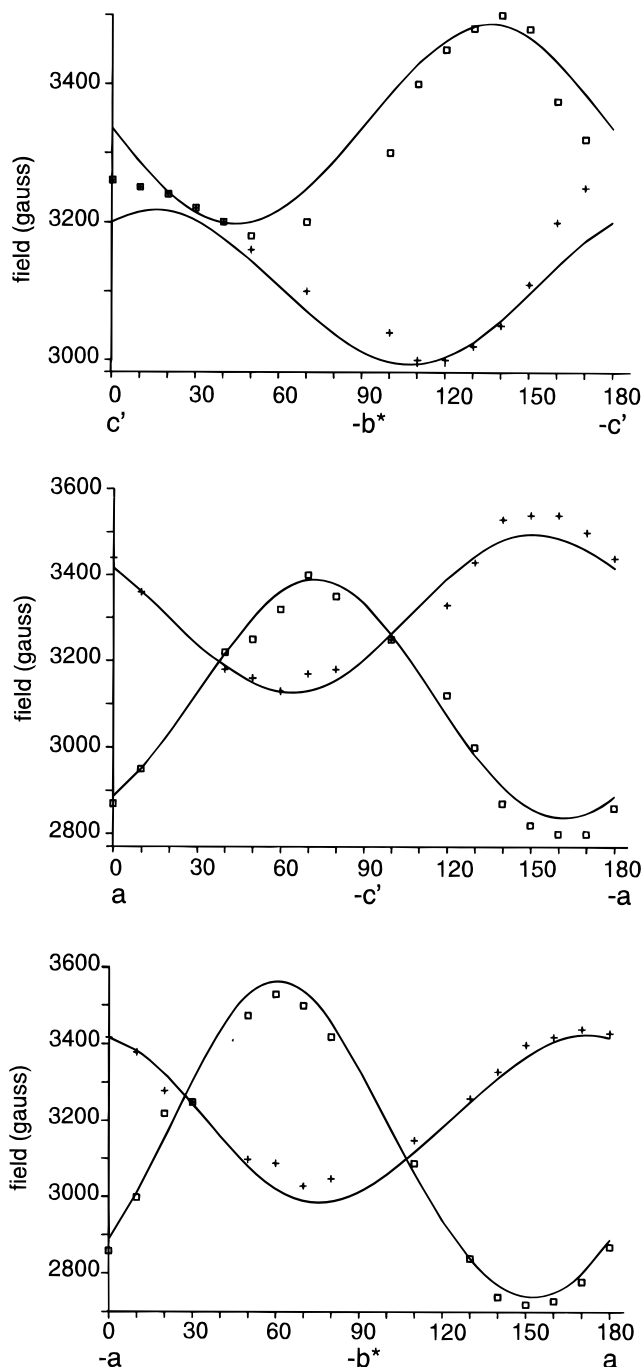


Figure 6. Angular dependence of the EPR transition fields for $[\text{Cu}_2(\text{biib})_2(\text{BF}_4)_2](\text{BF}_4)_2(\text{H}_2\text{O})_4$.

Table 5. Principal Values and Directions of \mathbf{g} and \mathbf{D} Tensors for $[\text{Cu}_2(\text{biib})_2(\text{BF}_4)_2] \cdot 2\text{BF}_4 \cdot 4\text{H}_2\text{O}$

$g_{xx} = 2.022(8)$	$g_{yy} = 2.060(7)$	$g_{zz} = 2.211(8)$
0.67(4)	-0.31(9)	-0.68(2)
0.53(6)	-0.43(8)	0.73(2)
0.51(11)	0.85(7)	0.13(4)
$D_{x'x'} = -0.0182(9)^a$	$D_{y'y'} = -0.081(6)^a$	$D_{z'z'} = +0.0264(7)^a$
0.93(1)	0.05(5)	0.37(1)
0.32(3)	0.39(3)	-0.86(1)
0.19(6)	-0.92(1)	-0.34(1)

^a In cm^{-1} .

Cu direction and an angle of *ca.* 23° with the normal to the least-squares plane provided by N(42), N(13), N(33), and N(23a). The zero-field splitting parameters are calculated as $D = 0.0396(14) \text{ cm}^{-1}$ and $E/D = 0.128$.²⁶

(24) Reedijk, J.; Nieuwenhuijse, B. *Recl. Trav. Chim. Pays-Bas* **1972**, *91*, 533.

(25) Mabbs, F. E.; Collison, D. *Electron Paramagnetic Resonance of d Transition Metal Compounds*; Elsevier: Amsterdam, 1992.

(26) Bencini, A.; Gatteschi, D. *EPR of Exchange Coupled Systems*; Springer-Verlag: Berlin, Heidelberg, Germany, 1990.

(27) Banci, L.; Bencini, A.; Gatteschi, D.; Zanchini, C. *J. Magn. Reson.* **1982**, *48*, 9.

(28) (a) Bencini, A.; Gatteschi, D.; Zanchini, C. *Inorg. Chem.* **1985**, *24*, 207. (b) Ajo, D.; Bencini, A.; Mani, F. *J. Inorg. Chem.* **1988**, *27*, 2437.

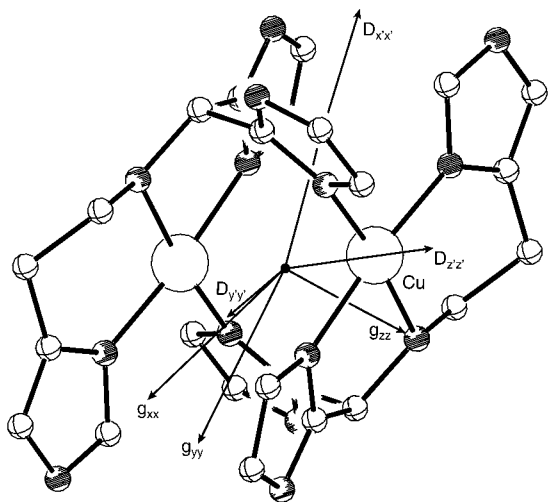


Figure 7. PLUTON²² projection showing the principal directions of the \mathbf{g} and \mathbf{D} tensors for $[\text{Cu}_2(\text{biib})_2(\text{BF}_4)_2](\text{BF}_4)_2(\text{H}_2\text{O})_4$.

The zero-field splitting tensor \mathbf{D} shows evidence of substantial exchange contributions.^{27,28} In fact, the largest component is not found to be parallel to the Cu–Cu direction, as would be expected for dominant dipolar effects. Upon substituting the g and D parameters obtained from the single-crystal EPR study in a simulation program,²⁹ assuming \mathbf{g} and \mathbf{D} coincident, the powder EPR spectrum was reproduced reasonably well.

Frozen Solution EPR Spectra. Except for the tribromocuprate(I) complex, well-resolved triplet spectra of the complexes are obtained from concentrated (0.01 M) frozen solutions in methanol/DMSO (77 K), showing that the dinuclearity of these complexes is fully preserved in this concentrated solution.^{24,25} The spectra show copper hyperfine interactions superimposed on the HZ absorptions with a value of $A = 85$ G. No variation of the zero-field splitting for the different complexes was observed in solution, indicating that in solution probably not the respective anion, but, instead, a solvent molecule is coordinated axially to the Cu(II) ion. The tribromocuprate(I) complex decomposes in solution, probably due to partial oxidation of the Cu(I) ions in the complex.

EPR spectra recorded at 77 K of frozen solutions of the perchlorate complex in methanol at various concentrations show that upon dilution the dinuclear complex reacts to form a mononuclear species with $g_{\perp} = 2.07$, $g_{\parallel} = 2.26$ and $A_{\parallel} = 150$ gauss. The structure of this mononuclear species is still unknown, but the g_{\parallel} and A_{\parallel} values indicate³⁰ that probably three nitrogens and one methanol solvent molecule are coordinated to the Cu(II) ion in this mononuclear species. The frozen-solution EPR spectra (77 K) of the perchlorate complex recorded at high concentration (0.01 M in methanol/DMSO) and at low concentration (2.10^{-4} in methanol) are shown in parts E and F of Figure 5, respectively.

Comparison of the EPR Parameters of the Four Complexes. Significant variations in the EPR zero-field splitting D of the complexes are observed, *i.e.* 0.058 cm^{-1} for the nitrate and perchlorate and 0.0396 cm^{-1} for the tetrafluoroborate complex. The zero-field splitting for the tribromocuprate(I) complex could not be determined.

The zero-field splitting parameter $D (= \frac{3}{2} D_{zz})$ for copper(II) dimers is determined by two main contributions:²⁶ A through-space magnetic dipolar interaction denoted as D^{dip}

Table 6. EPR Parameters of the Dinuclear Complexes

complex	g_x, g_y	g_{\parallel}	$ \mathbf{D} ^a$	$D^{\text{dip } a}$	$D^{\text{ex } a}$
BF_4^-	2.02, 2.06	2.21	0.0396	0.0788	-0.0392
ClO_4^-	2.02	2.21	0.058	0.0730	-0.0150
NO_3^-	2.02	2.21	0.058	0.0638	-0.0058

^a In cm^{-1}

between the unpaired electron spins and a through-bond anisotropic exchange interaction denoted as D^{ex} . The dipolar contribution D^{dip} to the zero-field splitting, which is expected to be parallel to the Cu–Cu direction can be calculated in the approximation of magnetic dipoles centered on the two metal ions²⁶ and is 0.0788 , 0.0730 , and 0.0638 cm^{-1} for the three complexes (BF_4^- , ClO_4^- , and NO_3^- , respectively) (Table 6). The variation of the experimentally determined zero-field splitting for the different complexes cannot be fully related to the change of the dipolar contribution to the zero-field splitting D . In the case of a pure dipolar interaction between the two copper(II) ions, the largest zero-field splitting is expected for the tetrafluoroborate complex. The exchange contributions to the zero-field splitting are calculated by the subtraction of the dipolar contribution from the experimentally determined D value, assuming that D and D^{dip} have the same sign ($D^{\text{ex}} = D - D^{\text{dip}}$), and are (BF_4^- , ClO_4^- , NO_3^-) -0.0392 , -0.0150 , and -0.0058 cm^{-1} , respectively (Table 5). These data seem to indicate a rapid decrease of the exchange component with increasing Cu–Cu distance.

Vis–Near-IR Spectra. The diffuse-reflectance spectra of the complexes in the Vis–near-IR region show a single band, as is usually observed for square-planar or square-pyramidal copper(II) complexes.^{23,30,31} The absorption maximum for the tetrafluoroborate and perchlorate complex is found at $17.70(5) \times 10^3 \text{ cm}^{-1}$. In the nitrate complex the band shifts to $17.60(5) \times 10^3 \text{ cm}^{-1}$ and in the tribromocuprate(I) complex to $17.50(5) \times 10^3 \text{ cm}^{-1}$. The position of the absorption maximum in the complexes is in agreement with the donor strength of the axially coordinated donor atom provided by the respective anion. Increasing donor strength of the axially coordinated anion causes a decrease of the d-orbital splitting between the d_{xz} , d_{yz} and $d_{x^2-y^2}$ orbitals, resulting in a small shift of the absorption maximum to lower energy.²³

Magnetic Measurements. The magnetic behavior of the perchlorate complex has been investigated in the temperature range 250–4.5 K. The magnetic susceptibility per copper(II) ion multiplied by the temperature (χT) is approximately $0.36 \text{ cm}^3 \text{ mol}^{-1} \text{ K}$ ($\mu_{\text{eff}} = 1.70$) over the whole temperature range and follows the Curie law corresponding to a single non-coupled electron spin ($S = \frac{1}{2}$).

Concluding Remarks

By comparison of the structural data of the four complexes a relationship could be established between the donor strength of the anion and some structural features of the complexes. The Cu(II)–Cu(II) distance, the distance of the copper(II) ion to the least-squares plane provided by N(13), N(42), N(33), and N(23)^a, and the distance between the two symmetry-related ($-x$, $-y$, $-z$) least-squares planes are correlated to the donor strength of the respective anion coordinated to the Cu(II) ions. The small structural differences between the perchlorate and tetrafluoroborate complex are probably caused by crystal packing effects and cannot be related to the small difference in binding strength of the respective anion coordinated to the copper ion.

(29) Neese, F.; Kroneck, P. M. H. The program EPR, Preliminary γ -test version 1.0, . . . 1994.

(30) Hathaway, B. J. *Comprehensive Coordination Chemistry*; Wilkinson, G., Gillard, R. D., McCleverty, J. A., Eds.; Pergamon Press: Oxford, U.K., 1987; Vol. 5, p 652.

(31) Lever, A. B. P. *Inorganic Electronic Spectroscopy*; Elsevier, Amsterdam: 1986.

The position of the absorption maximum in the Vis–near-IR region of the complexes is consistent with the donor strength of the axially coordinated donor atom provided by the respective anion.

A significant variation in the EPR zero-field splitting parameter D in the three dinuclear complexes is observed. The variation in D for the different complexes seems to be related to the small change of the Cu(II)–Cu(II) distance.

Frozen-solution EPR spectra of the perchlorate complex recorded at various concentrations in methanol show that upon dilution the dinuclear complex reacts to form a mononuclear species, in which probably three nitrogens and one solvent molecule are coordinated to the Cu(II) ion.

Further studies will deal with the reactivity of the present complexes toward azide, hydroxide, and hydrogen peroxide and of the Cu(I) complexes toward dioxygen.

Acknowledgment. We thank Bas de Vos and Reinier Tromp for the synthesis of the tribromocuprate(I) complex. Joachim Sinzig is acknowledged for his assistance with the magnetic susceptibility measurements. Roberta Sessoli and Fabrizio

Ferraro are acknowledged for assistance with the single-crystal EPR measurements and for stimulating discussions. Andrea Caneschi is acknowledged for orienting the single crystals. Financial support by the European Union, allowing regular exchange of preliminary results with several European colleagues, under contract ERBCHRXCT920014, is thankfully acknowledged. The authors are indebted to the EU for a grant as Host Institute in the EU Programme Human Capital and Mobility (1994–1997). This work was supported in part by the Netherlands Foundation of Chemical Research (SON) with financial aid from the Netherlands Organisation for Scientific Research (NWO).

Supporting Information Available: TME plots of $[\text{Cu}_2(\text{biib})_2(\text{BF}_4)_2](\text{BF}_4)_2(\text{H}_2\text{O})_4$ and $[\text{Cu}_2(\text{biib})_2(\text{NO}_3)_2](\text{NO}_3)_2(\text{H}_2\text{O})_4$ and tables giving further details of the structure determinations, including crystallographic data, atomic coordinates, bond lengths and angles, thermal parameters, and least-squares planes for all complexes (23 pages). Ordering information is given on any current masthead page.

IC951128Y